THE JOURNAL OF PHYSICAL CHEMISTRY A

Article

pubs.acs.org/JPCA

# Solvent Effect on the Stokes Shift and on the Nonfluorescent Decay of the Daidzein Molecular System

Yoelvis Orozco-Gonzalez, Carlos Bistafa, and Sylvio Canuto*

Instituto de Física, Universidade de São Paulo, CP 66318, 05314-970 São Paulo, SP, Brazil

Supporting Information

**ABSTRACT:** The flavonoids have been the target of several experimental works due to its influence in the human health as antioxidant elements. The fluorescence properties of these compounds have been widely studied due to the large Stokes shifts experimentally observed and the variety of processes that lead to the fluorescence. In the present work the role of the solvent in the large Stokes shift experimentally observed in the daidzein molecular system in water is theoretically studied. Also studied is the nonfluorescent decay mechanism in a polar aprotic solvent like acetonitrile. The solvent effect in the ground and in the low-lying excited electronic states is taken into account by using the sequential-QM/MM methodology. Excited state properties like equilibrium geometries and transition energies were studied by using multiconfigurational calculations, CASSCF and CASPT2. The excited electronic state responsible for the fluorescence spectrum in water was identified, and the large Stokes shift seems to be the result of the large interaction of the system in this electronic state with the solvent. On the other hand, spin−orbit coupling calculations, between the singlet and triplet electronic states, indicate favorable conditions for intersystem crossing, in agreement with the experimental result of nonfluorescence observation.

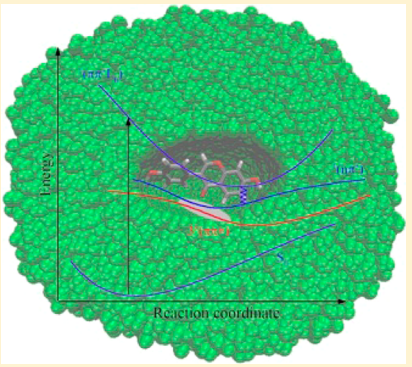


## 1. INTRODUCTION

The flavonoids are members of a family of polyphenolic compounds with antioxidant properties directly linked to health benefits[1−4] including a possible explanation for the French paradox.[5,6] Many studies[7−11] have suggested that the regular consumption of red wine could be the answer to the paradox, because the flavonoids are abundant in the seeds and skin of the grape and hence in the red wine.

For these and other reasons the flavonoids have been much studied. In particular, the fluorescence properties of these compounds have been the subject of several experimental works,[12−25] increasing the interest of theoretical studies of the excited states.[26−28] There is a wide variety of fluorescence characteristics of the flavonoids. Large Stokes shifts in solution have been observed in the 3-hydroxyflavones molecular systems (flavonols). The fluorescence, observed at about 500 nm, originates in an excited electronic state that is characterized by an intramolecular proton transfer from the 3-hydroxy group to the 4-carbonyl group.[12,16,18] Other systems characterized by the intramolecular excited-state proton transfer are the 5-hydroxyflavones, in which two emission bands were experimentally observed.[23] On the other hand, in the 7-hydroxyflavones, a large Stokes shift is also observed in alcohol and water, but this is not attributed to the intramolecular excited-state proton transfer. In these systems, two emission bands are normally observed in solution with pH higher than 2. The more intense is associated with the emission from the anionic form, and the weaker band is related to the keto tautomer. In solutions with pH less than 2, the fluorescence is associated to the zwitterionic form of the enol tautomer.[15,24,25]

The isoflavones are a subset of flavonoids, shown in Figure 1, that have deserved some experimental and theoretical attention.

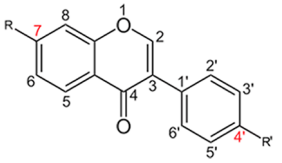


**Figure 1.** Representation of the isoflavones subset. For daidzein, the radicals are R = R′ = OH.

In a variety of these compounds, large Stokes shifts, on the order of 1.4 eV,[13,14,21,28] have been observed in the solvent environment. The fluorescence of these molecular systems have been observed in both basic and neutral conditions,[13,21,22] and no pH dependence has been obtained in some of them.[21] The experimental evidence concerning these compounds (see discussion in ref 28) indicate that the fluorescence can be assigned to the neutral forms.

In the present work we are particularly interested in the daidzein molecular system as a model compound. This is an isoflavone, as indicated in Figure 1, with R = OH and R′ = OH.

**Received:** March 3, 2013
**Revised:** May 3, 2013
**Published:** May 6, 2013






dx.doi.org/10.1021/jp4021646 | J. Phys. Chem. A 2013, 117, 4404−4411

Our interest in studying this molecular system arises from the necessity of a better understanding of the large Stokes shift values observed experimentally in the isoflavones subset.

The daidzein molecular system exhibits large Stokes shifts in polar protic solvents like water and methanol.[22,28] However, only a weak or nonfluorescence spectrum is detected when the daidzein is in a polar aprotic solvent like acetonitrile.[21,22] Hence, the aim of the present work is to theoretically elucidate the causes of the large Stokes shifts in polar protic solvents, such as water, and in addition to understand the nonfluorescent deactivation mechanism in acetonitrile. There is a recent and interesting theoretical work[28] that attempts to explain the role of the solvent in the photochemistry of isoflavones. There, analysis of the anomalous behavior is made using a simplified microsolvation model. In the present study we will consider a more realistic model for the solvent interaction with daidzein. Thus, Monte Carlo simulations of the liquid in the proper thermodynamic conditions are combined with quantum mechanics calculations to study the photophysics of this molecular system.

## 2. COMPUTATIONAL DETAILS

The energies of the low-lying excited electronic states of the daidzein were calculated using the multiconfigurational second-order perturbation theory (CASPT2),[29] based on the CASSCF reference wave function. In the CASSCF calculations, 12 electrons were correlated in 12 orbitals. The active orbitals are the five $\pi$ and six $\pi^*$ that better describe the three lowest $\pi\pi^*$ excited states and it was added the oxygen lone-pair orbital to describe the lowest $n\pi^*$ excited state. These active orbitals were selected by analyzing the contribution to the low-lying excited states in a previous multiconfigurational calculation that involved a higher active space, but only considering the single, double, triple, and quadruple excitations. It was used the ANO-L type basis set (atomic natural orbitals with Large primitive set), where the contraction scheme C, O (14s9p4d)/[4s3p1d], and H (8s4p)/[2s1p][30,31] has been used. This basis set yields converged results for the electronic transition energies, as verified in the early work of Roos and Fülscher.[32] The 1s core electrons of the oxygen and carbon atoms were kept frozen in the second-order perturbation step. In the CASSCF calculations, it was used the state average procedure, in which one single set of molecular orbitals is used to compute the five lowest roots.

The absorption transitions were studied using the ground electronic state equilibrium geometry optimized in the gas phase. This geometry was obtained at the MP2 level with the 6-31+G(d) basis set. The optimization was carried out with the Gaussian 03 program package.[33] The influence of the solvent in the ground state geometry was checked, using the polarizable continuum model (PCM)[34] model. In the case of both solvents considered, water and acetonitrile, the geometries are similar and do not differ much from that obtained in the gas phase. The major difference has been the change in the (2−3−1′−2′) dihedral angle from 49° in the gas phase to 57° and 56°, in acetonitrile and water, respectively. It is expected that the PCM could be a better approximation for the case of acetonitrile (nonprotic) than for water (protic solvent). To consider the protic aspect of water, we have also optimized the complex daidzein−water with one molecule of water attached to the oxygen atom of the C═O bond. As expected, in this case we find a stretch of the C═O bond length of 0.006 Å with the (2−3−1′−2′) dihedral of 50°, very close to that of the gas phase. The C═O stretch in the liquid should be smaller than this obtained in the minimum energy configuration. As expected,[35] this C═O bond stretch slightly decreases the $^1(n\pi^*)$ transition energy in water but these little modifications in the daidzein structure are not expected to change the qualitative conclusions regarding the radiative and nonradiative decays, so we only used the structure obtained in gas phase.

The study of the fluorescence spectrum was directed to identify the electronic state most populated in the absorption transitions and follow its behavior in solvent environment. The geometry optimizations of the excited electronic states were performed at the CASSCF level, considering the same active space and basis set discussed above. All multiconfiguration calculations were performed in the MOLCAS 7.4 program package.[36] The geometry optimizations of the excited states were performed for the isolated molecule.

Water and acetonitrile were the solvents considered in the present work, as used also in the experimental works. The solvent effect is taken into account using the sequential-QM/MM methodology.[37] Monte Carlo (MC) simulations were performed to generate solute−solvent configurations in the proper thermodynamic condition. These are then used in the quantum mechanical (QM) calculations of the electronic transitions. The MC simulations have been used as in previous applications in the ground electronic state[38,39] and also in the excited states.[40] We used the Metropolis sampling technique[41] in the *NPT* ensemble implemented in the DICE program.[42] In the simulations, one molecule of daidzein and 700 molecules of solvent were used in a cubic box with periodic boundary conditions and the image method,[41] at room conditions ($T$ = 25 °C and $P$ = 1 atm). The molecular interaction was described by the usual Lennard-Jones plus Coulomb potentials, with tree parameters for each atom $i$ ($\varepsilon_i$, $\sigma_i$, and $q_i$). The Lennard-Jones parameters are combined to generate the pair-potential parameters by $\varepsilon_{ij} = (\varepsilon_i\varepsilon_j)^{1/2}$ and $\sigma_{ij} = (\sigma_i\sigma_j)^{1/2}$. For daidzein in the ground and excited states, these parameters were obtained from Jorgensen's OPLS-AA force field.[43] For the water molecules the TIP3P model[44] was used and for acetonitrile the model proposed by Böhm and McDonald.[45] The atomic charges $q_i$ for daidzein in the ground and the excited electronic states have been obtained by taking into account the electronic polarization of each electronic state caused by the solvent.

The electronic polarization was considered by performing the iterative and sequential-QM/MM procedure previously described,[38,46,47] which brings the daidzein in the respective electronic state into electrostatic equilibrium with the solvent. Initially, the $q_i$ charges, obtained from the gas phase, were used in the MC simulation and the statistically uncorrelated configurations[48] of the liquid were selected to recalculate the new atomic charges and the solute dipole moment in the presence of the solvent. These QM calculations were performed with the daidzein embedded in the electrostatic field of the solvent using the average solvent electrostatic configuration (ASEC)[49] model. In the iteration, the calculated atomic charges of the solute are then updated in the Coulomb part of the potential for another MC simulation. This process is repeated until the convergence in the calculated dipole moment is obtained. The QM calculations of the solute dipole moments and charges were performed by using the electrostatic potential fitted (ESPF) method[50] implemented in MOLCAS 7.4.[36]

The total number of configurations generated in each MC simulation was $3.0 \times 10^5$, after $2.1 \times 10^8$ MC steps. After the


dx.doi.org/10.1021/jp4021646 | J. Phys. Chem. A 2013, 117, 4404−4411

convergence in the dipole moment, 100 statistically uncorrelated configurations were selected with less than 12% of statistical correlation for the QM calculation of the electronic transitions. In the absorption and emission energy calculation, the solvent was included by using the ASEC model.[49] ASEC accounts for all the solute−solvent electrostatic interactions, and a single QM calculation gives the same value as the average obtained with the entire ensemble.[49] In this model, after the MC simulation, statistically uncorrelated configurations are selected and used to construct an average configuration of the solvent, described as point charges. Explicit use of solvent molecules is not considered because of the very high computational effort involved.

To explain the inexistence of daidzein fluorescence in acetonitrile, the intersystem crossing transition was studied. In that sense, the spin−orbit coupling (SOC) elements between singlet and triplet electronic states were calculated by using the approximate one electron effective Hamiltonian[51] for the spin−orbit interaction. These calculations were performed using the RASSI (restricted active space state interaction) program[52] also implemented in MOLCAS 7.4.[36] The spin−orbit eigenstates are calculated in a variational way in the space spanned by the spin-free CASSCF wave functions, considering the spin−orbit interaction in the Hamiltonian. The dynamic correlation effects are included shifting the diagonal elements to the energies obtained in the CASPT2 calculations. The SOC strength between the involved electronic states (l, k) was evaluated as in ref 53:

$$\mathrm{SOC}_{\mathrm{lk}} = \sqrt{\sum_{u} |\langle T_{\mathrm{l},u}|\hat{H}_{\mathrm{SO}}|S_{\mathrm{k}}\rangle|^2} \quad (1)$$

where $u$ represents each spin component of the triplet state ($u = x, y, z$).

## 3. RESULTS AND DISCUSSION

**A. Absorption Spectrum.** The absorption spectra of daidzein molecular system in water and in acetonitrile were determined by using the ground electronic state optimized geometry, shown in Figure 2a. The dihedral angle between the chromone and the phenyl ring obtained in our optimization calculation is 49°, which is in reasonable agreement with the result of Beyhan et al.[28] of 39.9°, calculated at the CC2/aug-cc-pVDZ level of theory. The full information of the geometry can be found in the Supporting Information.

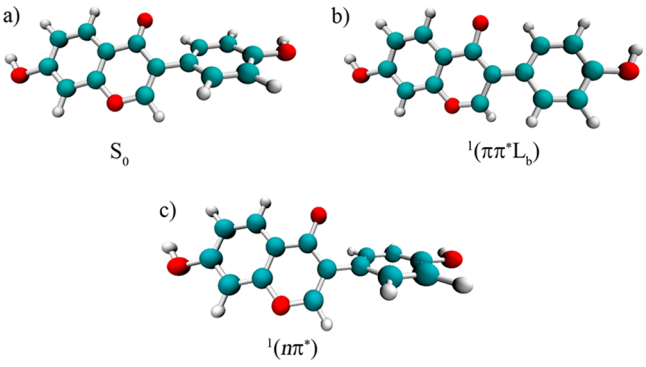


**Figure 2.** Optimized geometries of the corresponding electronic states.

To take into account the solvent effect in the absorption spectrum, the iterative procedure discussed in the previous section was performed to reach the solute−solvent electrostatic equilibrium of the daidzein in the ground electronic state. Parts a and b of Figure 3 show the convergence of the dipole moment in the iterative procedure for water and acetonitrile respectively, where the dipole moment of the ground state $S_0$ increases from 2.5 D in the gas phase to 10.0 D in water solution and to 3.8 D in acetonitrile.

In Table 1 are shown the four lowest excited electronic states calculated in solvent at CASPT2/ANO-L level. To distinguish the low-lying $\pi\pi^*$ electronic states, the Platt nomenclature was adopted,[54] where the $^1(\pi\pi^*\ L_a)$ state is mainly described by the HOMO (H) → LUMO (L) transition and $^1(\pi\pi^*\ L_b)$ by H−1 → L. The $^1(\pi\pi^*)$ electronic state is characterized by the HOMO−2 to LUMO transition, whereas the $^1(n\pi^*)$ is characterized by the transition from the oxygen lone-pair orbital to the LUMO. The molecular orbitals characterizing these electronic states are shown in Figure 4.

In the following, the results of the absorption transitions in water are discussed and subsequently those in acetonitrile. According to the results shown in Table 1, the calculated absorption spectrum in water shows two intense transitions, one due to the $^1(\pi\pi^*\ L_b)$ electronic state and the other to the $^1(\pi\pi^*\ L_a)$, with energies of 4.16 eV (298 nm) and 4.70 eV (264 nm), respectively. The first of these transitions is in excellent agreement with the experimental band observed with a maximum at 4.09 eV (303 nm) and used in the fluorescence excitation.[28] The second transition (4.70 eV) is in very good agreement with the experimental band witha maximum at about 5.00 eV (248 nm).[28] On the other hand, the fourth electronic transition shown, with an energy of 5.44 eV (228 nm), agrees with the experimental band that appears at the edge of the spectrum at about 5.85 eV (211 nm). Finally, the transition to the $^1(n\pi^*)$ electronic state, with an energy of 4.14 eV (300 nm) is not observed experimentally because it is weak and beneath an intense band.

The results obtained for the absorption in acetonitrile are also shown in Table 1. As can be seen, only one intense transition appears, given by the transition to the $^1(\pi\pi^*\ L_b)$ electronic state with an energy of 5.09 eV (244 nm). This transition is very close to the main band, experimentally observed with a maximum at 4.77 eV (260 nm). Another transition, to the $^1(\pi\pi^*\ L_a)$ electronic state, is obtained with lower intensity and energy of 4.37 eV (284 nm). This transition is close to a weak experimental band observed as a shoulder at 4.09 eV (303 nm).[28] It can be noted that these two electronic transitions are simultaneously displaced to the higher energetic region by about 0.3 eV (or 15 nm) in relation to the maxima of the experimental bands. This behavior may be due to the ASEC model used in the QM calculations, wherein only the electrostatic interaction with the solvent is considered and, perhaps, the exchange and van der Waals energies might be important for describing the interaction with the acetonitrile. The transition calculated at 5.76 eV (215 nm) corresponding to the $^1(\pi\pi^*)$ electronic state is in good agreement with the band observed at the edge of the spectrum at 5.85 eV (212 nm). Moreover, the $^1(n\pi^*)$ electronic state appears to be a dark state, indicated by the null oscillator strength.

**B. Fluorescence Spectrum in Water.** Based on the absorption spectrum of the daidzein, the emission spectrum description was oriented to the study of the $^1(\pi\pi^*\ L_b)$ excited state, because this state is most populated in the absorption transitions (Table 1) and reproduces very well the fluorescence excitation energy. In that way, the $^1(\pi\pi^*\ L_b)$ excited electronic


dx.doi.org/10.1021/jp4021646 | J. Phys. Chem. A 2013, 117, 4404−4411

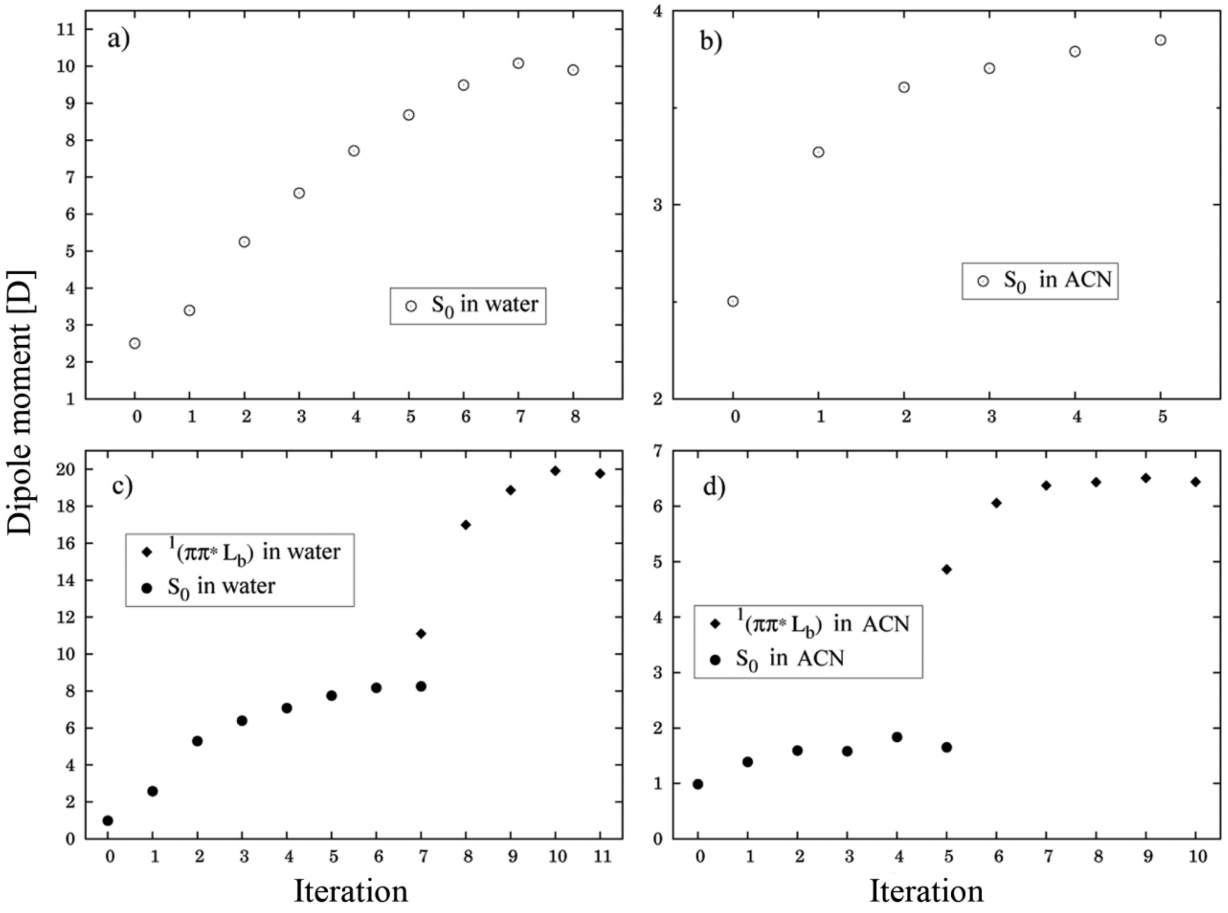


**Figure 3.** Changes of the dipole moment values of the corresponding electronic states in solvent, with respect to the number of iterations in the sequential-QM/MM procedure of solute electronic polarization. ACN means acetonitrile.

**Table 1. Absorption Energies to the Four Lowest Excited Electronic States in Water and in Acetonitrile and Emission Energy in Water[a]**

| Absorption | | | | | | | |
|---|---|---|---|---|---|---|---|
| water | | | | acetonitrile | | | |
| state | $E_{abs}$ | $f$ | $E_{abs}$[b] exp[28] | state | $E_{abs}$ | $f$ | $E_{abs}$[b] exp[28] |
| $^1(n\pi^*)$ | 4.14 | 0.070 | | $^1(n\pi^*)$ | 3.72 | 0.000 | |
| $^1(\pi\pi^* L_b)$ | 4.16 | 0.196 | 4.09 | $^1(\pi\pi^* L_a)$ | 4.37 | 0.077 | 4.09 |
| $^1(\pi\pi^* L_a)$ | 4.70 | 0.165 | 5.00 | $^1(\pi\pi^* L_b)$ | 5.09 | 0.305 | 4.77 |
| $^1(\pi\pi^*)$ | 5.44 | 0.057 | 5.85 | $^1(\pi\pi^*)$ | 5.76 | 0.027 | 5.85 |
| Emission in Water | | | | | | | |
| fluorescent state | | $E_{emi}$[c] | Stokes shift[d] | $E_{emi}$[b] exp[28] | | Stokes shift exp[28] | |
| $^1(\pi\pi^* L_b)$ | | 2.85/3.24 | 1.31/0.92 | 2.70 | | 1.40 | |

[a]The energetic values are indicated in eV. $f$ is the oscillator strength. [b]Energetic values corresponding to the experimental bands maxima. [c]Emission energy calculated in electrostatic equilibrium/nonequilibrium with the solvent. [d]Stokes shift calculated by using the absorption energy of the $^1(\pi\pi^* L_b)$ electronic state, which is the experimental fluorescence excitation, and the fluorescence energy obtained in electrostatic equilibrium/nonequilibrium with the solvent.

state was optimized at the CASSCF/ANO-L level. In this optimized geometry, shown in Figure 2b, the chromone and the phenyl ring approximate to a planar configuration (~14°, details can be found in the Supporting Information).

The solvation of the $^1(\pi\pi^* L_b)$ electronic state in water was studied in two stages. First, the lifetime of this electronic state is considered to be short and the solute−solvent electrostatic equilibrium is not reached. In that case, using the equilibrium geometry of the $^1(\pi\pi^* L_b)$ electronic state, solute−solvent configurations were obtained with the solvent in electrostatic equilibrium with the ground electronic state. That procedure is shown in Figure 3c by the circular points. The convergence of these points indicates the electrostatic equilibrium with the ground electronic state. Subsequently, an excited state lifetime large enough to reach the solute−solvent electrostatic equilibrium with the solvent is considered. That procedure is also shown in Figure 3c by the convergence of the diamond points. Splitting the iterative procedure in these two stages, it is possible to explicitly observe the electronic polarization corresponding to the excited electronic state once it is


dx.doi.org/10.1021/jp4021646 | J. Phys. Chem. A 2013, 117, 4404−4411

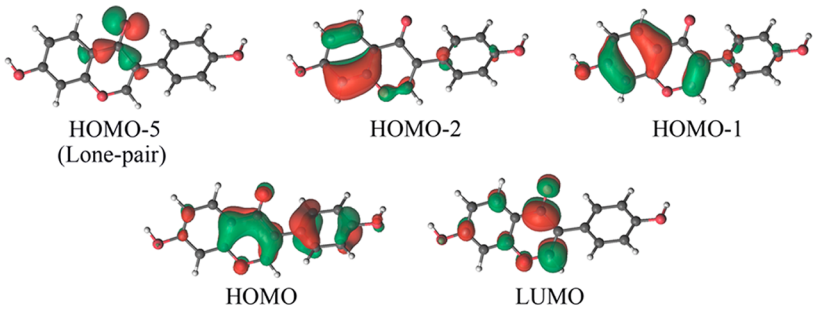


**Figure 4.** Representation of the molecular orbitals involved in the studied electronic transitions.

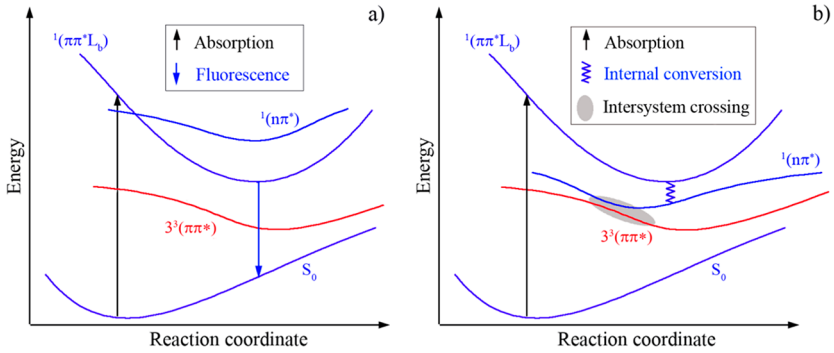


**Figure 5.** Schematic energetic profiles of the electronic states and deactivation mechanisms of the daidzein in water (a) and in acetonitrile (b).

populated. From Figure 3c, it can be seen that the electronic polarization of the $^1(\pi\pi^*\ L_b)$ excited electronic state, caused by the interaction with the solvent, increases the dipole moment from 11.1 to 19.8 D.

Both in the equilibrium condition and in the nonequilibrium, the $^1(\pi\pi^*\ L_b)$ electronic state is the lowest excited state, as shown schematically in Figure 5a. This electronic state stabilizes considerably due to the interaction with the water, whereas the $^1(n\pi^*)$ electronic state, which in the gas phase appears as the lowest one, is shifted to the blue.

The emission energies in water, calculated at the CASPT2/ANO-L level, are shown in Table 1. In the solute−solvent electrostatic nonequilibrium condition, the emission energy corresponding to the $^1(\pi\pi^*\ L_b)$ electronic state is 3.24 eV (383 nm). This leads to a Stokes shift value in water of 0.92 eV (85 nm) when compared with the absorption energy. Considering, as previously commented, that the $^1(\pi\pi^*\ L_b)$ excited-state lifetime is large enough to reach the solute−solvent electrostatic equilibrium, the calculated emission energy in water is 2.85 eV (435 nm). This result is in very good agreement with the experimental result of Beyhan et al.,[28] wherein the emission band is observed with a maximum at 2.67 eV (464 nm). In comparison with the absorption energy, a Stokes shift in water of 1.31 eV (137 nm) is obtained. That large Stokes shift value is in very good agreement with the experimental result of 1.40 eV.[28]

According to these results, the interaction with the solvent has great influence on the Stokes shift of the daidzein molecular system. We considered that the large electronic polarization of the $^1(\pi\pi^*\ L_b)$ excited electronic state, shown in Figure 3c, is the main cause of the large Stokes shift value experimentally observed, because it leads to a considerable energy stabilization of this electronic state. The deactivation mechanism of the daidzein in water, after the absorption transitions, is summarized in Figure 5a. It is interesting to mention that an electron density transfer can be seen resulting from the interaction of the system with the solvent. The electronic polarization caused by the solvent modifies the molecular orbitals (Figure 6), delocalizing the electronic density from the phenyl ring to the chromone.

**C. Suppression of the Fluorescence in Acetonitrile.** The fluorescence of the daidzein in polar aprotic solvent like acetonitrile is not observed experimentally. In this section we analyze this nonfluorescent decay and attempt a possible explanation.

According to the results shown in Table 1, the $^1(\pi\pi^*\ L_b)$ electronic state is the most populated in the absorption transitions. Hence, using the equilibrium geometry of this excited electronic state, the influence of the acetonitrile, as solvent, was considered in the low-lying excited states. As previously, the solvation of this electronic state was also studied in two stages. The electronic polarization of the $^1(\pi\pi^*\ L_b)$ electronic state, due to the interaction with acetonitrile, is weak, causing a small dipole moment change from 4.9 to 6.4 D. Because of this, the $^1(\pi\pi^*\ L_b)$ electronic state does not stabilize enough, being less stable than the $^1(n\pi^*)$ state, as shown schematically in Figure 5b.

In these conditions, according to the Kasha rule,[55] the system will decay by internal conversion from the $^1(\pi\pi^*\ L_b)$ electronic state to the $^1(n\pi^*)$. Therefore, to clarify the mechanism of the nonfluorescent decay of the daidzein, we studied the intersystem crossing between the $^1(n\pi^*)$ electronic state and the triplet states. The equilibrium geometry of the $^1(n\pi^*)$ electronic state was optimized at the CASSCF/ANO-L level, obtaining the geometry shown in Figure 2c, wherein the chromone and the phenyl ring form an angle of about 59°. In that geometry, the spin−orbit couplings between this electronic state and the closest triplet states were calculated. The results are shown in Table 2. The largest SOC value, equal to 42.5 $cm^{-1}$, is observed with the third triplet electronic state, $3^3(\pi\pi^*)$.


dx.doi.org/10.1021/jp4021646 | J. Phys. Chem. A 2013, 117, 4404−4411

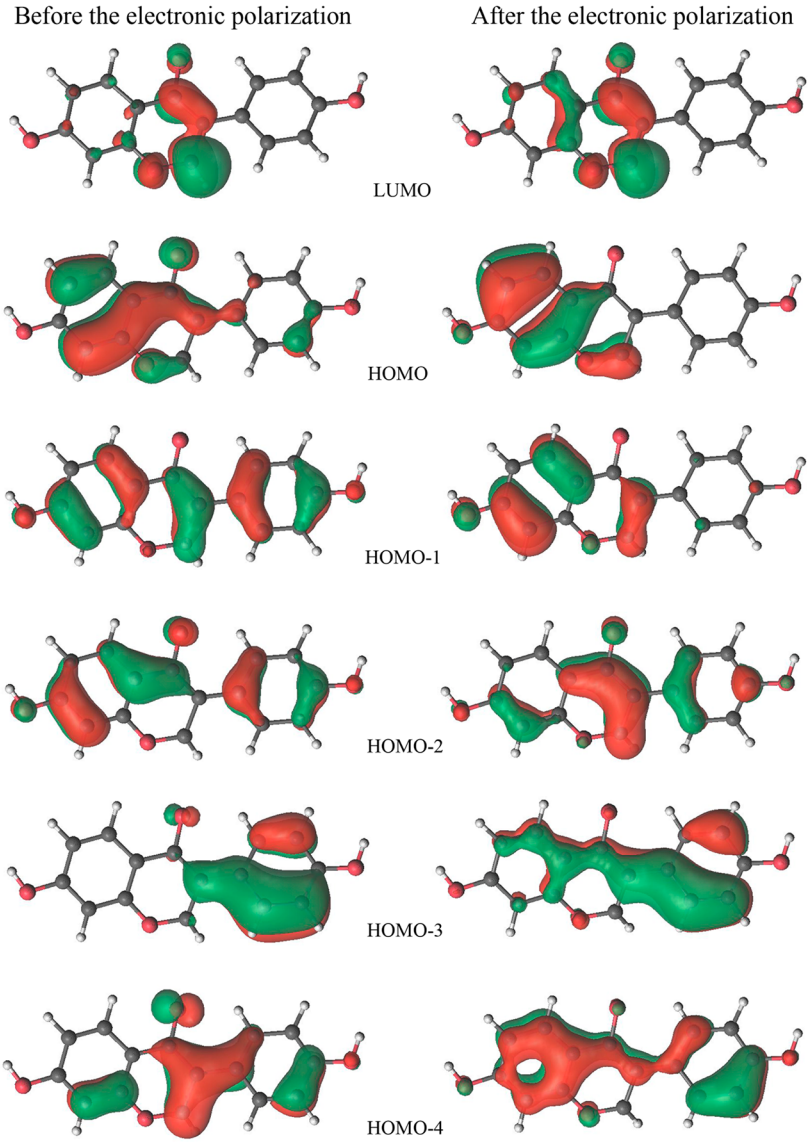


**Figure 6.** Changes in the molecular orbitals of the daidzein in the $^1(\pi\pi^*\ L_b)$ excited electronic state due to the electronic polarization caused by the water solvent.

**Table 2. Spin−Orbit Coupling Calculated Values and Energetic Gaps between the Considered Electronic States for Isolated Daidzein**

| state | | SOC ($cm^{-1}$) | $\Delta E^a$ (eV) |
|---|---|---|---|
| $^1(n\pi^*)$ | $1^3(\pi\pi^*)$ | 31.4 | −3.64 |
| | $2^3(n\pi^*)$ | | −0.29 |
| | $3^3(\pi\pi^*)$ | 42.5 | 0.20 |

[a]Energies compared to the $^1(n\pi^*)$ electronic state.

Although the energy of this electronic state appears 0.2 eV above the $^1(n\pi^*)$ state, this profile may be inverted in acetonitrile. We believe that, due to the weak interaction of the system with the acetonitrile, the $^1(n\pi^*)$ electronic state will be mildly shifted to the blue region whereas the $3^3(\pi\pi^*)$ state is shifted to the red, the triplet state remaining a little more stable than the singlet. The results shown in Table 2 are in excellent agreement with the El-Sayed rule,[56] which indicates that the intersystem crossing is allowed when the involved electronic states are of different spatial symmetries, like the $^1(n\pi^*)$ singlet state with the triplets $1^3(\pi\pi^*)$ and $3^3(\pi\pi^*)$. The SOC with the $2^3(n\pi^*)$ triplet state is negligible.

The intersystem crossing (ISC) rate is inversely proportional to the energy gap ($\Delta E$) between the electronic states and proportional to the SOC magnitude. The ISC rate is proportional to the following interaction factor:[57]

$$f_{SO} = \frac{SOC^2}{\Delta E^2} \quad (2)$$

Therefore, the large SOC value between the $^1(n\pi^*)$ and $3^3(\pi\pi^*)$ electronic states and the small energy gap between them can lead to an efficient intersystem crossing, preventing the fluorescent decay. This proposed deactivation mechanism of the daidzein in acetonitrile is summarized in the schematic representation shown in Figure 5b.

It is interesting to observe that different deactivation mechanisms depending on the solvent type were also experimentally observed in the 5-fluorouracil molecular system. In that system, it is experimentally observed that the fluorescent rate is much lower in acetonitrile than in water. The theoretical


dx.doi.org/10.1021/jp4021646 | J. Phys. Chem. A 2013, 117, 4404−4411

results of Improta et al.[58,59] indicate, in general, that in acetonitrile the n$\pi^*$ (dark) and $\pi\pi^*$ (bright) electronic states are very close energetically. Therefore, besides the fluorescence of the $\pi\pi^*$ electronic state, another deactivation mechanism appears through a conical intersection between these electronic states. This behavior is not observed in water because the n$\pi^*$ state is less stable than the $\pi\pi^*$.

## 4. CONCLUSIONS

The photophysics of the daidzein molecular system was theoretically studied in water and in acetonitrile. The absorption spectra were properly characterized in both solvents, but the electronic deactivation is different depending on the solvent type, as indicated in the experimental works. The obtained results are summarized in the schematic energetic profiles shown in Figure 5. The fluorescence mechanism of the daidzein in water, after the absorption transition, is shown in Figure 5a. The $^1$(n$\pi^*$) state, that in the gas phase and in acetonitrile is the lowest excited electronic state, is shifted to the blue region due to the interaction with water, whereas the $^1$($\pi\pi^*$ $L_b$) electronic state is energetically stabilized. The emission energy corresponding to this electronic state is in excellent agreement with the experimental results, as well as the calculated Stokes shift value.

In acetonitrile the picture is different, as indicated in Figure 5b. The $^1$($\pi\pi^*$ $L_b$) electronic state is the most populated in the absorption transitions. This electronic state in the equilibrium geometry is weakly solvated by the acetonitrile and does not stabilize enough. In the same way, the $^1$(n$\pi^*$) electronic state is mildly shifted to the blue and remains more stable energetically than the $^1$($\pi\pi^*$ $L_b$) state. The $^1$(n$\pi^*$) electronic state, which is populated by internal conversion according to the Kasha rule, shows very favorable conditions for an intersystem crossing with the $3^3$($\pi\pi^*$) electronic states. It can be concluded that the deactivation mechanism proposed in Figure 5b explains the nonfluorescent decay experimentally observed for the daidzein in acetonitrile. The deactivation mechanism of the triplet electronic states is still open for future investigation.

## ■ ASSOCIATED CONTENT

### Ⓢ Supporting Information

Optimized equilibrium geometries of the ground ($S_0$) and excited electronic states ($^1\pi\pi^*$ $L_b$ and $^1$n$\pi^*$). This material is available free of charge via the Internet at http://pubs.acs.org/.

## ■ AUTHOR INFORMATION

### Corresponding Author

*E-mail: canuto@if.usp.br.

### Notes

The authors declare no competing financial interest.

## ■ ACKNOWLEDGMENTS

This work has been partially supported by INCT-FCx, nBioNet, CNPq, CAPES and FAPESP (Brazil).

## ■ REFERENCES

(1) Shimoi, K.; Masuda, S.; Shen, B.; Furugori, M.; Kinae, N. Radioprotective Effects of Antioxidative Plant Flavonoids in Mice. *Mutat. Res., Fundam. Mol. Mech. Mutagen.*. **1996**, *350*, 153−161.

(2) Knekt, P.; Jarvinen, R.; Seppanen, R.; Heliovaara, M.; Teppo, L.; Pukkala, E.; Aromaa, A. Dietary Flavonoids and the Risk of Lung Cancer and Other Malignant Neoplasms. *Am. J. Epidemiol.* **1997**, *146*, 223−230.

(3) Monasterio, A.; Urdaci, M. C.; Pinchuk, I. V.; Lopez-Moratalla, N.; Martinez-Irujo, J. J. Flavonoids Induce Apoptosis in Human Leukemia U937 Cells through Caspase- and Caspase-Calpain-Dependent Pathways. *Nutr. Cancer* **2004**, *50*, 90−100.

(4) Terao, J.; Kawai, Y.; Murcita, K. Vegetable Flavonoids and Cardiovascular Disease. *Asia Pac. J. Clin. Nutr.* **2008**, *17*, 291−293.

(5) Renaud, S.; Delorgeril, M. Wine, Alcohol, Platelets, and the French Paradox for Coronary Heart-Disease. *Lancet* **1992**, *339*, 1523−1526.

(6) Tunstall-Pedoe, H.; Kuulasmaa, K.; Mahonen, M.; Tolonen, H.; Ruokokoski, E.; Amouyel, P.; Project, W. M. Contribution of Trends in Survival and Coronary-Event Rates to Changes in Coronary Heart Disease Mortality: 10-Year Results from 37 WHO MONICA Project Populations. *Lancet* **1999**, *353*, 1547−1557.

(7) Rosenkranz, S.; Knirel, D.; Dietrich, H.; Flesch, M.; Erdmann, E.; Böhm, M. Inhibition of the PDGF Receptor by Red Wine Flavonoids Provides a Molecular Explanation for the "French Paradox". *FASEB J.* **2002**, *16*, 1958−1960.

(8) Criqui, M. H.; Ringel, B. L. Does Diet or Alcohol Explain the French Paradox. *Lancet* **1994**, *344*, 1719−1723.

(9) Gronbaek, M.; Deis, A.; Sorensen, T. I. A.; Becker, U.; Schnohr, P.; Jensen, G. Mortality Associated with Moderate Intakes of Wine, Beer, or Spirits. *Br. Med. J.* **1995**, *310*, 1165−1169.

(10) Klatsky, A. L.; Armstrong, M. A.; Friedman, G. D. Red Wine, White Wine, Liquor, Beer, and Risk for Coronary Artery Disease Hospitalization. *Am. J. Cardiol.* **1997**, *80*, 416−420.

(11) Gronbaek, M.; Becker, U.; Johansen, D.; Gottschau, A.; Schnohr, P.; Hein, H. O.; Jensen, G.; Sorensen, T. I. A. Type of Alcohol Consumed and Mortality from All Causes, Coronary Heart Disease, and Cancer. *Ann. Intern. Med.* **2000**, *133*, 411−419.

(12) Sengupta, P. K.; Kasha, M. Excited-State Proton-Transfer Spectroscopy of 3-Hydroxyflavone and Quercetin. *Chem. Phys. Lett.* **1979**, *68*, 382−385.

(13) Wolfbeis, O. S.; Schipfer, R. Acidity Dependence of the Absorption and Fluorescence-Spectra of Isoflavone and 7-Hydroxyisoflavone. *Photochem. Photobiol.* **1981**, *34*, 567−571.

(14) Wolfbeis, O. S.; Furlinger, E.; Jha, H. C.; Zilliken, F. Absorption and Fluorescence of Isoflavones and the Effect of Shift Reagents. *Z. Naturforsch.* **1984**, *39b*, 238−243.

(15) Itoh, M.; Hasegawa, K.; Fujiwara, Y. 2-Step Laser Excitation Fluorescence Study of the Ground-State and Excited-State Proton-Transfer in Alcohol-Solutions of 7-Hydroxyisoflavone. *J. Am. Chem. Soc.* **1986**, *108*, 5853−5857.

(16) Mcmorrow, D.; Kasha, M. Intramolecular Excited-State Proton-Transfer in 3-Hydroxyflavone - Hydrogen-Bonding Solvent Perturbations. *J. Phys. Chem.* **1984**, *88*, 2235−2243.

(17) Sarkar, M.; Guha Ray, J.; Sengupta, P. K. Luminescence Behaviour of 7-Hydroxyflavone in Aerosol OT Reverse Micelles: Excited-State Proton Transfer and Red-Edge Excitation Effects. *J. Photochem. Photobiol. A.* **1996**, *95*, 157−160.

(18) Schwartz, B. J.; Peteanu, L. A.; Harris, C. B. Direct Observation of Fast Proton-Transfer - Femtosecond Photophysics of 3-Hydroxyflavone. *J. Phys. Chem.* **1992**, *96*, 3591−3598.

(19) Ameer-Beg, S.; Ormson, S. M.; Brown, R. G.; Matousek, P.; Towrie, M.; Nibbering, E. T. J.; Foggi, P.; Neuwahl, F. V. R. Ultrafast Measurements of Excited State Intramolecular Proton Transfer (Esipt) in Room Temperature Solutions of 3-Hydroxyflavone and Derivatives. *J. Phys. Chem. A* **2001**, *105*, 3709−3718.

(20) Bader, A. N.; Ariese, F.; Gooijer, C. Proton Transfer in 3-Hydroxyflavone Studied by High-Resolution 10 K Laser-Excited Shpol'skii Spectroscopy. *J. Phys. Chem. A* **2002**, *106*, 2844−2849.

(21) de Rijke, E.; Joshi, H. C.; Sanderse, H. R.; Ariese, F.; Brinkman, U. A. T.; Gooijer, C. Natively Fluorescent Isoflavones Exhibiting Anomalous Stokes' Shifts. *Anal. Chim. Acta* **2002**, *468*, 3−11.

(22) Dunford, C. L.; Smith, G. J.; Swinny, E. E.; Markham, K. R. The Fluorescence and Photostabilities of Naturally Occurring Isoflavones. *Photochem. Photobiol. Sci.* **2003**, *2*, 611−615.

(23) Chou, P. T.; Chen, Y. C.; Yu, W. S.; Cheng, Y. M. Spectroscopy and Dynamics of Excited-State Intramolecular Proton-Transfer Reaction in 5-Hydroxyflavone. *Chem. Phys. Lett.* **2001**, *340*, 89−97.
(24) Sarkar, M.; Sengupta, P. K. Luminescence Behaviour of 7-Hydroxyflavone: Temperature-Dependent Effects. *J. Photochem. Photobiol. A* **1989**, *48*, 175−183.
(25) Schipfer, R.; Wolfbeis, O. S.; Knierzinger, A. Ph-Dependent Fluorescence Spectroscopy 0.12. Flavone, 7-Hydroxyflavone, and 7-Methoxyflavone. *J. Chem. Soc., Perkin Trans. 2.* **1981**, 1443−1448.
(26) Prasad, De, S.; Ash, S.; Bar, H.; Kumar Bhui, D.; Dalai, S.; Misra, A. Excited State Intramolecular Proton Transfer in 5-Hydroxy Flavone: A DFT Study. *J. Mol. Struct.: THEOCHEM.* **2007**, *824*, 8−14.
(27) Marian, C. M. Spin-Forbidden Transitions in Flavone. *Spectrochim. Acta Part A.* **2009**, *73*, 1−5.
(28) Beyhan, S. M.; Gotz, A. W.; Ariese, F.; Visscher, L.; Gooijer, C. Computational Study on the Anomalous Fluorescence Behavior of Isoflavones. *J. Phys. Chem. A* **2011**, *115*, 1493−1499.
(29) Andersson, K.; Malmqvist, P. A.; Roos, B. O. 2nd-Order Perturbation-Theory with a Complete Active Space Self-Consistent Field Reference Function. *J. Chem. Phys.* **1992**, *96*, 1218−1226.
(30) Widmark, P. O.; Malmqvist, P. A.; Roos, B. O. Density-Matrix Averaged Atomic Natural Orbital (Ano) Basis-Sets for Correlated Molecular Wave-Functions 0.1. 1st Row Atoms. *Theor. Chim. Acta* **1990**, *77*, 291−306.
(31) Widmark, P. O.; Joakim, B.; Persson; Roos, B. O. Density-Matrix Averaged Atomic Natural Orbital (Ano) Basis-Sets for Correlated Molecular Wave-Functions 0.2. 2nd Row Atoms. *Theor. Chim. Acta* **1991**, *79*, 419−432.
(32) Fulscher, M. P.; Roos, B. O. The Excited-States of Pyrazine - a Basis-Set Study. *Theor. Chim. Acta* **1994**, *87*, 403−413.
(33) Frisch, M. J.; Trucks, G. W.; Schlegel, H. B.; Scuseria, G. E.; Robb, M. A.; Cheeseman, J. R.; Montgomery, J. A., Jr.; Vreven, T.; Kudin, K. N.; Burant, J. C.; et al. *Gaussian 03*, Revision D.01; Gaussian Inc.: Wallingford, CT, 2004.
(34) Tomasi, J. Thirty Years of Continuum Solvation Chemistry: A Review, and Prospects for the near Future. *Theor. Chem. Acc.* **2004**, *112*, 184−203.
(35) Coutinho, K.; Saavedra, N.; Canuto, S. Theoretical Analysis of the Hydrogen Bond Interaction between Acetone and Water. *J. Mol. Struct.: THEOCHEM.* **1999**, *466*, 69−75.
(36) Karlström, G.; Lindh, R.; Malmqvist, P.-Å.; Roos, B. O.; Ryde, U.; Veryazov, V.; Widmark, P. O.; Cossi, M.; Schimmelpfennig, B.; Neogrady, P.; et al. *Molcas: A Program Package for Computational Chemistry*; Lund University: Lund, Sweden, 2003.
(37) Canuto, S. *Solvation Effects on Molecules and Biomolecules: Computational Methods and Applications*; Springer: London, 2008.
(38) Georg, H. C.; Coutinho, K.; Canuto, S. Converged Electronic Polarization of Acetone in Liquid Water and the Role in the n-$\pi^*$ Transition. *Chem. Phys. Lett.* **2006**, *429*, 119−123.
(39) Fonseca, T. L.; Georg, H. C.; Coutinho, K.; Canuto, S. Polarization and Spectral Shift of Benzophenone in Supercritical Water. *J. Phys. Chem. A* **2009**, *113*, 5112−5118.
(40) Orozco-Gonzalez, Y.; Coutinho, K.; Peon, J.; Canuto, S. Theoretical Study of the Absorption and Nonradiative Deactivation of 1-Nitronaphthalene in the Low-Lying Singlet and Triplet Excited States Including Methanol and Ethanol Solvent Effects. *J. Chem. Phys.* **2012**, *137*, 054307−8.
(41) Allen, M. P.; Tildesley, D. J. *Computer Simulation of Liquids*; Clarendon Press: Oxford, U.K., 1987.
(42) Coutinho, K.; Canuto, S. *Dice: A Monte Carlo Program for Molecular Liquid Simulations*; University of São Paulo: São Paulo, 2009.
(43) Jorgensen, W. L.; Maxwell, D. S.; Tirado-Rives, J. Development and Testing of the OPLS All-Atom Force Field on Conformational Energetics and Properties of Organic Liquids. *J. Am. Chem. Soc.* **1996**, *118*, 11225−11236.
(44) Jorgensen, W. L.; Chandrasekhar, J.; Madura, J. D.; Impey, R. W.; Klein, M. L. Comparison of Simple Potential Functions for Simulating Liquid Water. *J. Chem. Phys.* **1983**, *79*, 926−935.
(45) Bohm, H. J.; McDonald, I. R.; Madden, P. A. An Effective Pair Potential for Liquid Acetonitrile. *Mol. Phys.* **1983**, *49*, 347−360.
(46) Kongsted, J.; Osted, A.; Mikkelsen, K. V.; Christiansen, O. The QM/MM Approach for Wavefunctions, Energies and Response Functions within Self-Consistent Field and Coupled Cluster Theories. *Mol. Phys.* **2002**, *100*, 1813−1828.
(47) Martin, M. E.; Sanchez, M. L.; del Valle, F. J. O.; Aguilar, M. A. A Multiconfiguration Self-Consistent Field/Molecular Dynamics Study of the $(n\text{-}\pi^*)^1$ Transition of Carbonyl Compounds in Liquid Water. *J. Chem. Phys.* **2000**, *113*, 6308−6315.
(48) Coutinho, K.; Canuto, S.; Zerner, M. C. A Monte Carlo-Quantum Mechanics Study of the Solvatochromic Shifts of the Lowest Transition of Benzene. *J. Chem. Phys.* **2000**, *112*, 9874−9880.
(49) Coutinho, K.; Georg, H. C.; Fonseca, T. L.; Ludwig, V.; Canuto, S. An Efficient Statistically Converged Average Configuration for Solvent Effects. *Chem. Phys. Lett.* **2007**, *437*, 148−152.
(50) Ferré, N.; Ángyán, J. G. Approximate Electrostatic Interaction Operator for QM/MM Calculations. *Chem. Phys. Lett.* **2002**, *356*, 331−339.
(51) Hess, B. A.; Marian, C. M.; Wahlgren, U.; Gropen, O. A Mean-Field Spin-Orbit Method Applicable to Correlated Wavefunctions. *Chem. Phys. Lett.* **1996**, *251*, 365−371.
(52) Malmqvist, P. A.; Roos, B. O. The CASSCF State Interaction Method. *Chem. Phys. Lett.* **1989**, *155*, 189−194.
(53) Merchan, M.; Serrano-Andres, L.; Robb, M. A.; Blancafort, L. Triplet-State Formation Along the Ultrafast Decay of Excited Singlet Cytosine. *J. Am. Chem. Soc.* **2005**, *127*, 1820−1825.
(54) Platt, J. R. Classification of Spectra of Cata-Condensed Hydrocarbons. *J. Chem. Phys.* **1949**, *17*, 484−495.
(55) Kasha, M. Characterization of Electronic Transitions in Complex Molecules. *Discuss. Faraday Soc.* **1950**, 14−19.
(56) El-Sayed, M. A. Spin-Orbit Coupling and the Radiationless Processes in Nitrogen Heterocyclics. *J. Chem. Phys.* **1963**, *38*, 2834−2838.
(57) Turro, N. J. *Modern Molecular Photochemistry*; University Science Books: Sausalito, CA, 1991.
(58) Gustavsson, T.; Sarkar, N.; Lazzarotto, E.; Markovitsi, D.; Barone, V.; Improta, R. Solvent Effect on the Singlet Excited-State Dynamics of 5-Fluorouracil in Acetonitrile as Compared with Water. *J. Phys. Chem. B* **2006**, *110*, 12843−12847.
(59) Santoro, F.; Barone, V.; Gustavsson, T.; Improta, R. Solvent Effect on the Singlet Excited-State Lifetimes of Nucleic Acid Bases: A Computational Study of 5-Fluorouracil and Uracil in Acetonitrile and Water. *J. Am. Chem. Soc.* **2006**, *128*, 16312−16322.